Supersonic radiative heat waves in low-density high-Z material

J. Massen,[1] G. D. Tsakiris,[1] K. Eidmann,[1] I. B. Földes,[1,*] Th. Löwer,[1] R. Sigel,[1]
S. Witkowski,[1] H. Nishimura,[2] T. Endo,[3] H. Shiraga,[2] M. Takagi,[2] Y. Kato,[2] and S. Nakai[2]
[1]*Max-Planck-Institut für Quantenoptik, D-85748 Garching, Germany*
[2]*Institute of Laser Engineering, Osaka University, Suita Osaka, 565 Japan*
[3]*Institute for Laser Technology, 2-6 Yamada-oka, Suita, Osaka, 565 Japan*
(Received 23 February 1994)

The propagation of a radiation heat wave through lead-doped foam with a density of 80 mg/cm^3 was experimentally investigated. The wave is driven by 100–150 eV *Hohlraum* radiation generated in 1–3 mm diam gold cavities heated by a 2.5 kJ, 0.8 ns laser pulse (wavelength 0.35 μm). The propagation velocity was obtained from the delayed onset of intense thermal emission from the rear side of the foam sample. The results agree with theoretical predictions for a nonablative heat wave and with numerical simulations, and indicate that the radiation heat wave propagates with a velocity that is larger than the sound velocity in the heated foam.

PACS number(s): 52.50.Jm, 44.40.+a, 47.70.Mc

It has been recently demonstrated [1] that by depositing the energy of modern high-power lasers in small gold cavities it is possible to establish thermal x-ray fluxes of the order 10^{14} to 10^{15} W/cm^2. At these x-ray fluxes, plasma at high temperatures is produced in which energy transport occurs predominantly via radiative heat conduction. Marshak [2] was the first to study the diffusion of such an intense thermal flux into the matter under the condition of local thermodynamic equilibrium (LTE) between radiation and matter, and he found that it leads to the formation of a radiation heat wave.

The behavior of radiatively heated matter driven by intense energy fluxes is well described in the book by Zel'dovich and Raizer [3]. First, a supersonic heat wave is formed which propagates into the undisturbed material. In time, due to the increasing mass of heated material, it slows down and eventually is overtaken by a shock wave, thus becoming of the ablative type. Normally, at solid densities, the very early nonablative stage does not play an important role since its duration is usually in the picosecond range. However, by lowering the density of the x-ray heated material, it is possible to extend considerably this early nonablative period. It turns out that if the material opacity exhibits a weak dependence on density, the total mass of heated material does not change with density. This means that a decrease in density will result in a higher heat wave velocity. In contrast, the sound velocity, which depends only on the mean thermal ion velocity, is not affected by a density variation. The consequence of a higher heat wave velocity and a constant sound velocity is a longer temporal window during which the heat wave remains nonablative and supersonic. In the experiments described here, by lowering the density of the radiatively heated material by more than two orders of magnitude relative to solid state density, it was possible to extend this pure nonablative period into the nanosecond range and observe the radiatively driven supersonic heat wave. It should be noted here that the propagation of supersonic heat waves has been observed previously only in xenon gas [4].

This gives rise to very interesting prospects in connection with experiments where the heating of material at high temperatures without hydrodynamic motion offers ideal conditions. For example, in x-ray spectroscopy and opacity measurements [5–8] one would like to perform experiments with a plasma free of density and temperature gradients. Furthermore, low-density material, usually called foam, has come to play an important role as an efficient converter with minimum hydro-losses in the concept of heavy ion inertial fusion [9]. A number of applications, the most notable of which is the laser driven inertial confinement fusion, require very uniform irradiation conditions (1–2%) [10–12]. Low-density high-Z doped material can be used to smooth out irradiation nonuniformities in the soft x-ray range since it decouples the hydromotion from the diffusive energy transport via radiation [13].

We present here results from experiments with high-Z doped foam obtained through polymerization of the organometallic monomer *p*-Trimethylleadstyrene [14]. The objective was to measure the speed with which the heat wave propagates in this low-density high-Z material. The most suited method for this purpose was judged to be the radiative burnthrough of various foam thicknesses. This type of measurement has been successfully applied to solid density gold foils where the delay in the arrival of the burnthrough signal was detected [15,16]. The main difference between solid density and foam burnthrough is the speed with which the heat wave propagates through the material.

The nonablative heat wave propagation is described by the nonlinear radiative heat conduction equation [3]. In order to obtain an analytical expression for the propaga-

*Permanent address: Research Institute for Particle and Nuclear Physics, P.O. Box 49, H-1525 Budapest, Hungary.

tion of the heat wave front we assume a power law dependence on temperature and density for the Rosseland mean opacity $\kappa_R = AT^S\rho^R$ and similarly for the internal energy $\epsilon=\alpha T^{k+1}$ of the heated material. The general case where the specific heat is temperature dependent ($k\neq 0$) can be treated if one writes (as suggested in Ref. 3) the nonlinear heat conduction equation in terms of the specific energy $E=\rho\epsilon$ instead of temperature, i.e.,

$$\frac{\partial E}{\partial t}=a'\nabla\cdot(E^{n'}\nabla E)\ , \tag{1}$$

where $n'=(n-k)/(k+1)$ and

$$a'=\tfrac{16}{3}\sigma A^{-1}[1/(k+1)]\alpha^{-(n+1)/(k+1)} \times\rho^{-(n+1)/(k+1)-(R+1)}\ .$$

For nonlinear radiative heat conduction $n=3-S$ and σ is the Stefan-Boltzmann constant. The scaling law for the heat wave front position x_h is obtained from Eq. (1) by replacing the derivatives by their corresponding ratios, i.e., the energy conservation gives $E/t\sim S_0/x_h$ and the heat flux diffusion $S_0\sim a'E^{n'+1}/x_h$. As boundary condition here we assume a given constant source flux S_0 externally supplied to the heated material. By combining the two relations one arrives at the following scaling law for the heat wave front: $x_h\sim t^{(n'+1)/(n'+2)}S_0^{n'/(n'+2)}a'^{1/(n'+2)}$. We specialize now this scaling law for the lead-carbon mixture in the foam material employed in the experiments. We estimate the Rosseland mean opacity of the mixture by adding the frequency dependent opacities for carbon and lead, taking into account the mass fraction of the components (35% lead, 65% styrene). The individual frequency dependent opacities for the components are calculated in the average ion approximation [17]. By integrating over frequency the appropriately weighted sum of the components, the Rosseland mean opacity of the mixture is found to be $\kappa_R=4.4\times10^6T^{-1.57}\rho^{0.1}$. In this expression κ_R is in cm^2/g, T in eV, and ρ in g/cm^3. In an analogous manner, we estimate the internal energy of the foam mixture by addition of the mass weighted internal energy of the components, which we take from the SESAME tables [18]. This procedure gives the following approximate scaling law for the internal energy: $[\epsilon\ (\mathrm{erg/g})]=4.05\times10^{11}T^{1.2}$. For these special values for the Rosseland mean opacity and internal energy one obtains $n'=3.64$ and $a'=B\rho^{-5.74}$, with $B=1.43\times10^{-48}$. The scaling law for the heat wave front position (with the density dependence explicitly included) is then $x_h=ct^{0.82}S_0^{0.65}B^{0.18}\rho^{-1.02}$, where c is a proportionality factor of the order of 1, x_h in cm, t in s, and S_0 in erg/(cm^2 s). It is seen that the heat wave velocity $c_h=dx_h/dt$ scales as $\sim t^{-0.18}S_0^{0.65}\rho^{-1.02}$, i.e., the heat wave front propagates faster in lower densities and for higher fluxes while it slows down slightly with time. To obtain quantitative results for the nonablative heat wave burnthrough one has to determine the proportionality factor c. This was accomplished by numerically solving the energy relation in Eq. (1). The boundary condition employed in the numerical solution was a given net heat flux input, S_0, into the material, i.e., $S_0=S_i-\sigma T^4$. Here, S_i is the externally supplied incident flux and σT^4 represents the radiation losses due to the boundary temperature T. The numerical solution confirms the scaling relation obtained analytically and gives a value for the proportionality factor $c\simeq0.8$. To assess the effects of the hydrodynamic motion, we have performed simulations using our hydrodynamics computer code MULTI [19]. In addition to seeing the effect of the hydrodynamic motion on the heat wave propagation at the low density of the foam, such simulations can deal with the real pulse shape, provide a more detailed description of radiative transport (multigroup diffusion approximation), and include the process of laser-light conversion to x rays. In the one-dimensional (spherical) simulations a laser-irradiated gold sphere is located in the center of the cavity. Its surface area corresponds to the laser irradiated wall area in the experiment to warrant the correct laser intensity, which determines the conversion efficiency and the source spectrum. The thickness and density of the cavity wall were chosen equal to our foam samples. Because of the lack of frequency dependent opacity tables for lead we have performed our simulations with a fictitious gold foam. Our average ion calculations [17] have shown that replacing the lead content in the mixture by gold leaves the Rosseland mean opacity practically unchanged. For the internal energy of the foam material we interpolated the SESAME tables' values for the components, gold and carbon, taking into account their mass fraction. The radiation losses through holes are included by an appropriate boundary condition at the innermost Lagrangian cell of the wall [20].

The experiments were carried out with one bundle of five frequency tripled ($\lambda=0.35$ μm) beams of the GEKKO XII Nd-glass-laser facility. The maximum energy of 2.5 kJ was delivered in a pulse of 0.8–0.9 ns duration. The experiments were performed with flattened *Hohlraum* targets (see Fig. 1) optimized to avoid direct and specularly reflected laser light irradiation of the foam

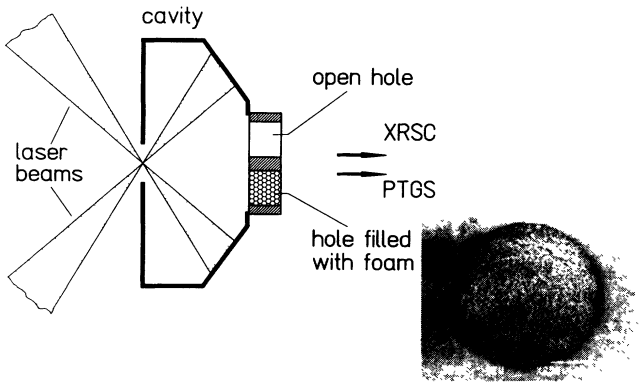

FIG. 1. Schematic diagram showing a cross-sectional view of the special type of flattened cavities made out of gold and their heating method. The cover plate attached to the rear side of the cavity and the viewing direction of the two diagnostics are also indicated. Inset: a scanning electron microscope photograph of a cover plate hole filled with foam.

samples and to minimize the total wall area. They had an opening at the rear side where the cover plates were mounted. The cover plates were circular gold plates with two diagnostic holes, a larger one filled with foam and a smaller one for the time fiducial. The diameter of each diagnostic hole was appropriately dimensioned to take into account the expected difference in intensity. To avoid the observation of hard radiation coming from the gold edges or direct radiation passing through some gaps between the foam and the gold wall, the foam holes were covered by a plastic mask with a hole 100 μm smaller in diameter than the foam hole itself. The thickness of the plates determined the thickness of the foam samples. The experiments were carried out with three cavity sizes equivalent to a 1, 2, and 3 mm diameter sphere total wall area. For each target type we measured a mean brightness temperature of 150, 120, and 100 eV respectively, with an accuracy of ± 5 eV. Foam plate thicknesses of 50, 75, 100, 150, 200, and 300 μm were used. The foam density reached was ≈ 80 mg/cm^3. Chemical analysis using UV-spectroscopy of a foam sample yielded a mass fraction for lead of about $35\% \pm 5\%$. This value was used in our estimates. To our knowledge, this is the only foam material available that meets the experimental requirements of high-Z doping, density less than 100 mg/cm^3, and inhomogeneities in the range of a few micrometers, i.e., small compared with the extent of the heat wave. A scanning electron microscope photograph of a foam sample is presented in the inset of Fig. 1, where the extent of the foam planarity and granularity can be seen.

The temporal evolution of the radiation from the hole filled with foam and from the open reference hole was measured simultaneously at a fixed wavelength using a soft x-ray streak camera (XRSC). The experimental arrangement was similar to the one used in the observation of the heat wave burnthrough in solid density foils [16]. The observation wavelength was 60 Å, the bandwidth ~ 15 Å, and the temporal resolution ≤ 30 ps. Time-integrated, space-resolved spectra from both holes were obtained in the range 5–100 Å with the help of a pinhole transmission-grating spectrometer (PTGS), which used absolute calibrated x-ray film as a detector. The brightness temperature of the cavity radiation was measured with a second diagnostic set at an angle of 90° to our main set, consisting of an XRSC in combination with a slit transmission grating, recording the time-resolved spectra and a PTGS for absolute calibration.

A typical data set of our burnthrough diagnostic, the XRSC traces that represent the spatially and temporally resolved emission from the diagnostic holes, is given in Fig. 2. As can be clearly seen there is a typical delay between the signal of the reference hole and the foam signal. It is interpreted as the so-called burnthrough time, i.e., the transit time required by the radiation heat wave to propagate through the foam. Comparing the burnthrough signals of foam with that from solid foils [15,16], we see that the onset of the radiation intensity of the foam is not as steep as it is for a foil. This can be attributed to the special spectral features of the carbon-lead mixture of which the foam consists and which become apparent in spectrally resolved foam burnthrough mea-

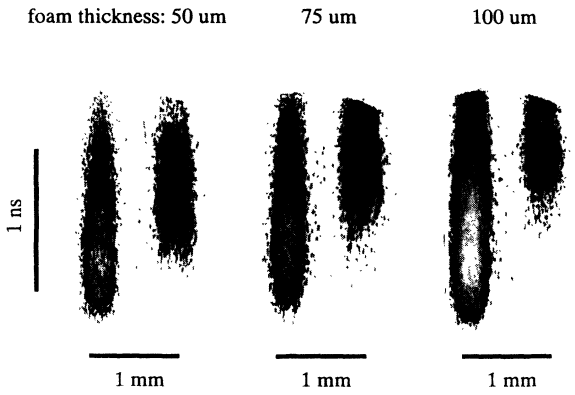

FIG. 2. Raw data of the XRSC records showing the delay in arrival of the heat wave (right trace) traveling through the indicated thickness of foam material with respect to the radiation emanating from the open hole (left trace). The foam was irradiated with an x-ray flux having a radiation temperature of $T_R \sim 100$ eV (3 mm targets).

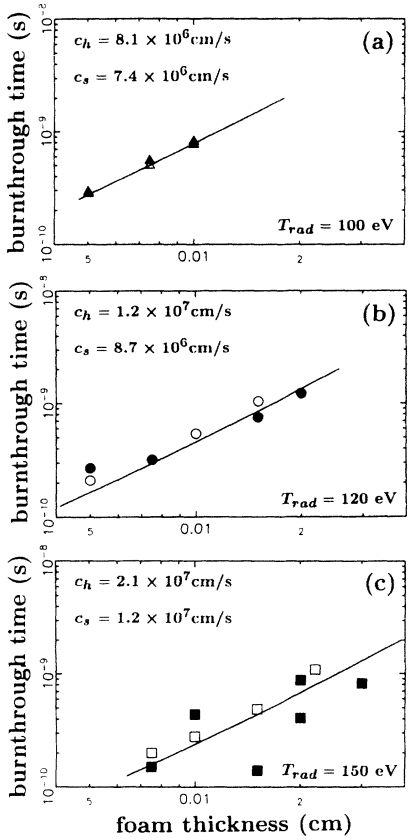

FIG. 3. The burnthrough time as a function of the foam sample thickness for the (a) 3 mm, (b) 2 mm, and (c) 1 mm in diameter *Hohlraum* targets. The experimentally measured radiation temperature T_R for each case is given. The experimental points are represented by full symbols, while the open symbols represent the simulation results. The solid line depicts the numerical solution of the diffusion equation for the nonablative heat wave [Eq. (1)]. The mean heat wave velocity c_h and the corresponding sound velocity c_s as obtained from the simulations for the three cases are also given.

surements. These data we obtained from another experiment, where an x-ray driven foam foil was observed by the temperature diagnostic set, which records the time resolved burnthrough spectra. Unlike solid density gold, the foam exhibits a transmission window for wavelengths shorter than 20 Å, where the radiation is transmitted through the foam nearly instantaneously. This transmission window in the harder x-ray range leads to a nonnegligible preheating of the foam, which results in the observed smoothing of the burnthrough front. But it also contributes to a reduction of the foam granularity by homogenizing it before the arrival of the heat wave.

For the interpretation of our burnthrough results we present in Fig. 3 a comparison of the experimental data with the numerical solution of Eq. (1) and the simulations using the computer code MULTI. Within the experimental scatter of the data, there is a very good agreement for the burnthrough time as a function of the foam thickness between experimental points and numerical scaling, as well as simulation points. Furthermore, it is seen that the simulation results reproduce the numerical solution of Eq. (1), indicating that the hydromotion of the radiatively heated foam is negligible and does not play an important role at these densities.

The sound and the heat wave velocities from the simulation results are given in Fig. 3 for the three different size targets. The heat wave appears to be supersonic in all three cases. Whereas in the 3 mm cavities heated to a lower temperature the supersonic character of the heat wave is marginal, for the higher temperatures prevailing in the 1 mm cavities the heat wave becomes almost twice as fast as the compression wave.

In conclusion, it could be shown that with the laser energies and foam densities available today the nonablative range in which a radiatively driven heat wave propagates in an undistributed material is achievable. The results demonstrate the possibility of investigating pure radiation diffusion (free of hydromotion) in the high temperatures range (100–200 eV). Such studies are of interest for obtaining a basic insight into the state of matter at very high temperatures and have potential applications for inertial fusion and for opacity measurements.

This work was supported in part by the Commission of the European Communities in the framework of the Association Euratom-Max-Planck-Institut für Plasmaphysik and by the Monbusho International Scientific Research Program.

[1] See, for example, R. Sigel, in *Handbook of Plasma Physics, Vol. 3: Physics of Laser Plasma,* edited by A. M. Rubenchik and S. Witkowski (Elsevier Science, New York, 1991), p. 163 and references therein.
[2] R. E. Marshak, Phys. Fluids **1**, 24 (1958).
[3] Ya. B. Zel'dovich and Yu. P. Raizer, *Physics of Shock Waves and High-Temperature Hydrodynamic Phenomena* (Academic, New York, 1966).
[4] J. C. Bozier *et al.*, Phys. Rev. Lett. **57**, 1304 (1986).
[5] S. J. Davidson *et al.*, Apply. Phys. Lett. **52**, 847 (1988).
[6] T. S. Perry *et al.*, Phys. Rev. Lett. **67**, 3784 (1991).
[7] L. B. Da Silva *et al.*, Phys. Rev. Lett. **69**, 438 (1992).
[8] W. Schwanda and K. Eidmann, Phys. Rev. Lett. **69**, 3507 (1992).
[9] M. M. Basko and J. Meyer-ter-Vehn, Nucl. Fusion **33**, 601 (1993).
[10] R. L. McCrory and C. P. Verdon, in *Inertial Confinement Fusion,* Proceedings of the Course and Workshop of the International School of Physics Piero Caldirola, Varenna, 1988, edited by A. Caruso and E. Sindoni (Editrice Compositori, Bologna, 1989), p. 183.
[11] S. Atzeni, Europhys. Lett. **11**, 639 (1990).
[12] B. A. Remington *et al.*, Phys. Rev. Lett. **67**, 3259 (1991).
[13] M. Murakami (unpublished).
[14] J. G. Noltes, H. A. Budding, and G. J. M. Der Kerk, Rec. Trav. Chim. Pays-Bas. **79**, 1076 (1960).
[15] R. Sigel *et al.*, Phys. Rev. Lett. **65** (5), 587 (1990).
[16] R. Sigel *et al.*, Phys. Rev. A **45** (6), 3987 (1992).
[17] G. D. Tsakiris and K. Eidmann, J. Quant. Spectrosc. Radiat. Transfer **38**, 353 (1987).
[18] B. I. Bennet, J. D. Johnson, G. I. Kerley, and G. T. Rood, Los Alamos National Laboratory Report No. LA-7130, 1978 (unpublished); W. F. Huebner *et al.* (T4-group), Los Alamos National Laboratory Report No. LALP-83-4, 1983 (unpublished).
[19] R. Ramis, R. Schmalz, and J. Meyer-ter-Vehn, Comput. Phys. Commun. **49**, 475 (1988).
[20] J. Massen, G. D. Tsakiris, and R. Sigel, Phys. Rev. E **48**, 2073 (1993).

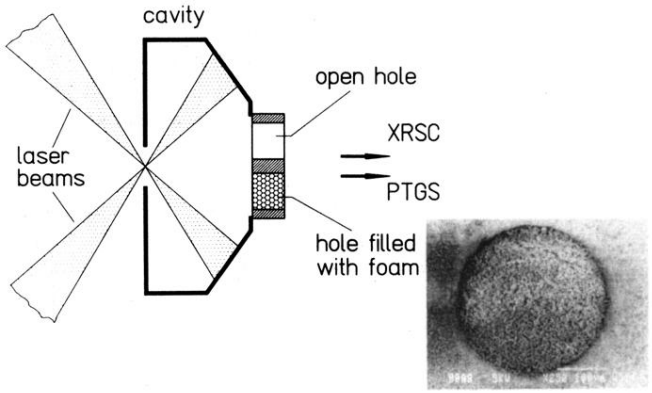

FIG. 1. Schematic diagram showing a cross-sectional view of the special type of flattened cavities made out of gold and their heating method. The cover plate attached to the rear side of the cavity and the viewing direction of the two diagnostics are also indicated. Inset: a scanning electron microscope photograph of a cover plate hole filled with foam.

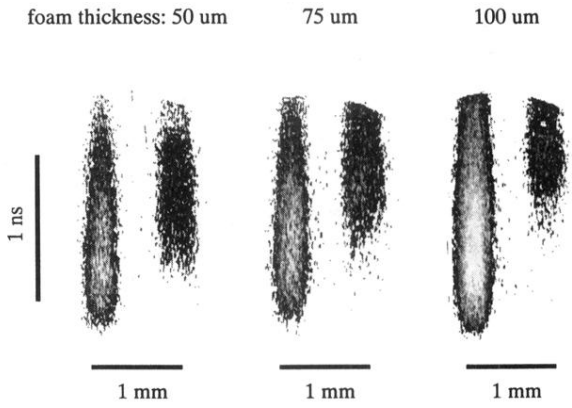

FIG. 2. Raw data of the XRSC records showing the delay in arrival of the heat wave (right trace) traveling through the indicated thickness of foam material with respect to the radiation emanating from the open hole (left trace). The foam was irradiated with an x-ray flux having a radiation temperature of $T_R \sim 100$ eV (3 mm targets).